International Journal of Non-Linear Mechanics 47 (2012) 699–711

Contents lists available at SciVerse ScienceDirect

International Journal of Non-Linear Mechanics

journal homepage: www.elsevier.com/locate/nlm

Non-linear buckling analysis of inclined circular cylinder-in-cylinder by the discrete singular convolution

Z. Yuan, X. Wang*

State Key Laboratory of Mechanics and Control of Mechanical Structures, Nanjing University of Aeronautics and Astronautics, No. 29 Yudao Street, Nanjing 210016, China

ARTICLE INFO

Article history:
Received 18 July 2011
Received in revised form
18 November 2011
Accepted 25 November 2011
Available online 8 December 2011

Keywords:
Discrete singular convolution
Lateral buckling
Helical buckling
Inclined cylinder

ABSTRACT

The lateral buckling and helical buckling problem of a circular cylinder constrained by an inclined circular cylinder under a compressive force, torsion, and its own weight is complicated and difficult to obtain an exact analytical solution. Thus, the non-linear differential equation is solved incrementally using the discrete singular convolution (DSC) algorithm together with the Newton–Raphson method. Detailed formulations are worked out. A simple way to numerically simulate the helical buckling is proposed and solution procedures are given. Four examples with various inclined angles, weights per unit length of the inner cylinder, axial applied loads, and boundary conditions are investigated. To verify the formulations and solution procedures, comparisons are firstly made with data obtained using the finite element method. It is verified that under certain circumstance, only lateral or helical buckling alone will occur. On some other circumstance, both lateral buckling and helical buckling may occur and the critical helical buckling loads are higher than the critical lateral buckling loads if frictions are not considered. Some conclusions are made based on the results presented herein.

1. Introduction

The buckling behavior of a circular cylinder constrained in a circular cylinder subjected to axial compression, torsion, and gravitational loads is of interest to engineering practice, for example, to the oil industry [1–4]. Buckling may initiate in a lateral mode that snakes along the lower surface of the constraining cylinder. With the increase of axial compressive force, the inner cylinder may achieve an overall helically buckled state in which the buckled cylinder forms a helix spiraling around the inner surface of the constraining cylinder. The progression on this subject is clear from past research, but this has been scattered over many papers. Recently, Wicks et al. [5] gave an excellent review on the development of this subject.

Due to the outer cylinder constraint and gravitational loads, as well as the effect of the boundary conditions, the buckling behavior of short cylinders is even more complicated and difficult to obtain an exact analytical solution. It is also seen that how the initiating lateral mode transitions to the helical mode, especially for the short cylinders, still unclear, since little experimental data exist on constrained cylinder buckling [4,5]. Therefore, approximate and numerical methods, such as the Rayleigh–Ritz technique, the Galerkin method, the finite element method (FEM), and the differential quadrature element method (DQEM), are the appropriate approaches to obtain solution to the complicated problem. Huang and Pattillo [3] used the Rayleigh–Ritz technique the helical buckling of a tube in an inclined wellbore. Mitchell [1] used the Galerkin method to study the effects of well deviation on the helical buckling behavior. Power's method together with the method of the steepest decent was used to solve the non-linear algebraic equations. Based on the numerical results, stability criteria were developed for lateral and helical buckling. Liu and Wang [6] developed a special 2-node-4-dof beam element and studied the non-linear buckling behavior of tubing in deviated wells by FEM. The Newton–Raphson method with small disturbances was used to solve the non-linear algebraic equations. Munteanu and Barraco [7] developed a special 3-node-3-dof beam element and investigated the non-linear buckling behavior of a pipe in horizontal pipe by employing the FEM. Gravitational load was neglected for simplicity and the Newton–Raphson method was used to solve the non-linear algebraic equations. The helical buckling configurations were clearly shown. Gan et al. [8] employed the differential quadrature element method combined with the incremental iterative method to study the buckling behavior of tubular in deviated wells. It is observed [6,8] that the tubular would lose contact with the well-wall to transit from the lateral buckling mode to the helical buckling mode.

It is seen that if the gravitational load is considered, the corresponding load can be only obtained approximately using numerical integration if the local methods are used [1,6]. On the

* Corresponding author.
E-mail address: wangx@nuaa.edu.cn (X. Wang).

0020-7462/$ - see front matter © 2011 Elsevier Ltd. All rights reserved.
doi:10.1016/j.ijnonlinmec.2011.11.008

other hand, in the global method, such as the differential quadrature method, difficulties may arise in modeling long tubes with large number of grid points and in modeling the discontinuity of the slope existing in the helical buckling. Thus the differential quadrature element method has to be used [8] to overcome these difficulties. The discrete singular convolution (DSC) algorithm, proposed by Wei [9], possesses both the accuracy of global methods and the flexibility of local methods. The DSC algorithm has been successfully used in applications of many mechanical problems [10] and similar solution accuracy as to DQM is observed [11]. The method has been successfully used in solving the challenge problems of vibration analysis of plates with irregular internal supports and mixed boundary conditions [12–15], vibrating at higher-order modes [16], free vibration, and stability analysis of arbitrary straight-sided quadrilateral plates, such as skew, trapezoidal, and rhombic plates [17,18]. More recently, the non-linear static analysis of plates was analyzed using the DSC algorithm [19–21]. Therefore, the DSC algorithm may be an excellent alternative to solve the complicated buckling problem of constrained cylinders.

The objective of the present work is to investigate the nonlinear buckling behavior of a circular cylinder constrained in a rigid circular cylinder subjected to axial compression and gravitational loads using the DSC algorithm. A simple way to initiate the lateral and helical buckling modes is proposed to study how the initiating lateral and helical modes. Detailed formulations and solution procedures are given. The non-regularized Lagrange's delta sequence kernel (DSC-LK) [11,13] is used. Four examples with various inclined angles, weights per unit length of the inner cylinder, axial applied loads and boundary conditions are investigated. To verify the formulations and solution procedures, comparisons are firstly made with data obtained using the finite element method. It is verified that under certain conditions, only lateral or helical buckling alone will occur [1]. On some other conditions, both lateral buckling and helical buckling may occur and the critical helical buckling loads are higher than the critical lateral buckling loads if frictions are not considered. Some conclusions are drawn based on the results presented herein.

2. Basic equations

Consider a circular cylinder constrained by an inclined rigid circular cylinder, shown in Fig. 1. The material of the inner cylinder is isotropic. The length, weight per unit length, and bending rigidity of the inner cylinder are L, EI, and q, respectively. The inner cylinder is subjected to a compressive force P at its upper end and a resulting compressive force F_b at its lower end. r is the radial clearance between inner and outer cylinders, α is the inclined angle, W_n is the contact force per unit length, and θ is the deviation angle in the xy plane. The inner cylinder contacts initially with the outer cylinder shown in Fig. 1. For convenience, the origin of a right-handed Cartesian coordinate system is at the upper end, x and y axes are in the cross-section plane, and z axis coincides with the axis of outer cylinder. Frictions between the inner and outer cylinders are not considered.

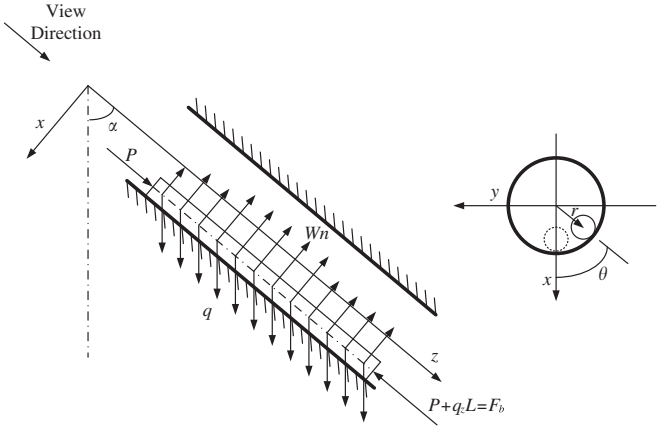

Fig. 1. Schematic diagram of a tube sitting in an inclined rigid cylinder.

Compared to the length of the inner cylinder, r is usually very small, thus small displacement is assumed. The deformed shape of the inner cylinder can be conveniently described by the Euler–Rodrigues quaternion $\boldsymbol{l}$, defined by [7,22]:

$$\mathbf{l}=(l_0,l_1,l_2,l_3)^T=\left(1,\frac{\varphi n_x}{2},\frac{\varphi n_y}{2},\frac{\varphi n_z}{2}\right)^T=\left(1,\frac{\varphi_x}{2},\frac{\varphi_y}{2},\frac{\varphi_z}{2}\right)^T \tag{1}$$

where φ is the magnitude of the rotation vector $\varphi\boldsymbol{n}$, n_x,n_y,n_z are the direction cosines of the unit vector $\boldsymbol{n}$.

In terms of the Euler–Rodrigues quaternion, the curvature can be expressed by [7,22]

$$\boldsymbol{\kappa}=\mathbf{G}\mathbf{l}' \tag{2}$$

where

$$\mathbf{G}=2\begin{bmatrix}-l_1 & l_0 & l_3 & -l_2\\ -l_2 & -l_3 & l_0 & l_1\\ -l_3 & l_2 & -l_1 & l_0\end{bmatrix}=\begin{bmatrix}-\varphi_x & 2 & \varphi_z & -\varphi_y\\ -\varphi_y & -\varphi_z & 2 & \varphi_x\\ -\varphi_z & \varphi_y & -\varphi_x & 2\end{bmatrix} \tag{3}$$

and

$$\mathbf{l}'=\begin{pmatrix}0 & \frac{1}{2}\frac{d\varphi_x}{ds} & \frac{1}{2}\frac{d\varphi_y}{ds} & \frac{1}{2}\frac{d\varphi_z}{ds}\end{pmatrix}^T \tag{4}$$

where s is the curvilinear coordinate along the deformed axis of the inner cylinder.

To calculate the displacement components from $(\varphi_x,\varphi_y,\varphi_z)$, the rotation matrix is needed. Fig. 2 shows an original straight cylinder deformed into a curved one. A typical point T on the initial configuration has been turned to t on the current configuration, and $\mathbf{G}_i$ and $\mathbf{g}_i$ are the reference coordinates at point T and t. The unit vector $\mathbf{G}_3$ ($\mathbf{g}_3$) is along the tangent direction and $\mathbf{G}_1$, $\mathbf{G}_2$ ($\mathbf{g}_1$, $\mathbf{g}_2$) are perpendicular to $\mathbf{G}_3$ ($\mathbf{g}_3$). According to the Euler–Rodrigues quaternion, the rotation matrix between $\mathbf{g}_i$ and $\mathbf{G}_i$ can be expressed as [7,22]

$$\mathfrak{R}_{gG}=\begin{bmatrix}2(l_0^2+l_1^2)-1 & 2(l_1l_2-l_0l_3) & 2(l_1l_3+l_0l_2)\\ 2(l_1l_2+l_0l_3) & 2(l_0^2+l_2^2)-1 & 2(l_2l_3-l_0l_1)\\ 2(l_1l_3-l_0l_2) & 2(l_2l_3+l_0l_1) & 2(l_0^2+l_3^2)-1\end{bmatrix} \tag{5}$$

Thus

$$\begin{Bmatrix}u\\ v\\ w\end{Bmatrix}=\begin{Bmatrix}u\\ v\\ w\end{Bmatrix}_o+\int_0^s\mathbf{g}_3ds=\begin{Bmatrix}u\\ v\\ w\end{Bmatrix}_o+\int_0^s\mathfrak{R}_{gG}\mathbf{G}_3ds$$
$$=\begin{Bmatrix}u\\ v\\ w\end{Bmatrix}_o+\int_0^s\begin{Bmatrix}\varphi_y+\frac{1}{2}\varphi_x\varphi_z\\ -\varphi_x+\frac{1}{2}\varphi_y\varphi_z\\ 1-\frac{1}{2}(\varphi_x^2+\varphi_y^2)\end{Bmatrix}ds \tag{6}$$

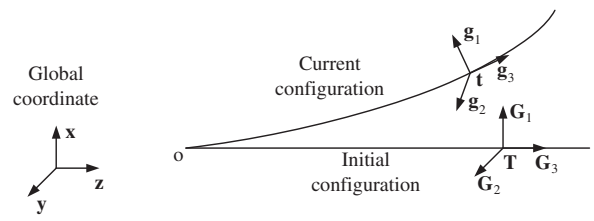

Fig. 2. Sketch of the reference coordinate systems.